Density Functional Calculation of the Electronic Circular Dichroism Spectra of the Transition Metal Complexes [M(phen) 3] 2+ (M = Fe, Ru, Os)

ARTICLE *in* THE JOURNAL OF PHYSICAL CHEMISTRY A · JUNE 2005

Impact Factor: 2.69 · DOI: 10.1021/jp0444363 · Source: PubMed

4 AUTHORS, INCLUDING:

Boris Le Guennic
Université de Rennes 1
137 PUBLICATIONS **2,365** CITATIONS

SEE PROFILE

Density Functional Calculation of the Electronic Circular Dichroism Spectra of the Transition Metal Complexes $[M(phen)_3]^{2+}$ (M = Fe, Ru, Os)

Boris Le Guennic,[‡,†] Wolfgang Hieringer,[§] Andreas Görling,[§] and Jochen Autschbach*[,‡]

Department of Chemistry, University at Buffalo, Buffalo, New York 14260-3000, and Lehrstuhl für Theoretische Chemie, Universität Erlangen, Egerlandstrasse 3, D-91058 Erlangen, Germany

Received: December 7, 2004; In Final Form: March 30, 2005

The circular dichroism spectra of the tris-bidentate metal complexes Λ-$[M(phen)_3]^{2+}$, with M = Fe, Ru, Os and phen = 1,10-tris-phenanthroline, are investigated computationally, employing time-dependent density functional theory. Good agreement with experimental spectra is obtained for Ru and Os. The Λ-$[Os(phen)_3]^{2+}$ spectrum is analyzed in detail. It is shown how relativistic effects red shift CD bands where the Os 5d-orbital participates to a large extent in the excitations. Further, the participation of the metal in the ligand $\pi \rightarrow \pi^*$ exciton CD is determined to be of the order of 10%. Though solvent effects can have a noticeable effect on individual transitions and rotatory strengths, they are demonstrated to have only a very small overall effect on the resulting simulated CD spectra. For Λ-$[Fe(phen)_3]^{2+}$, the results are shown to be rather sensitive to the choice of the applied hybrid and nonhybrid density functionals, and the optimized geometries based thereupon. In particular, the sign pattern of the lower-energy part (up to 33×10^3 cm^{-1}) of the Λ-$[Fe(phen)_3]^{2+}$ CD spectrum is difficult to reproduce. Some combinations of functionals and geometries yield good agreement with experiment, but no "best" approach can be devised based on the available results. Possible sources of errors in the spectrum of Λ-$[Fe(phen)_3]^{2+}$ due to deficiencies in the functionals and the exchange-correlation kernels are investigated.

1. Introduction

Because of the presence of chiral molecules in living organisms, optical activity is an important topic in chemistry and biochemistry. Electronic circular dichroism (CD), which measures the difference of absorption of left and right circularly polarized light, has turned out to be a powerful tool, which provides information on both the origin of the optical activity and the electronic and geometric structure of chiral molecules.[1−5] Since many transition metal complexes are chiral, CD spectroscopy is a very useful experimental method employed in the characterization of such compounds as well.[6−8]

Theoretical approaches are very helpful in the assignment and the interpretation of the CD spectra of chiral metal complexes.[9−14] Several decades ago, crystal field models were developed to describe the d-to-d transitions at the metal center (see refs 6, 7, 15, 16, and references therein). The exciton coupling model was applied to excitations occurring within the ligands of chiral metal complexes[17−20] and has been instrumental for the assignment of absolute configurations, for instance of tris-phenanthroline and tris-bipyridyl complexes, before single-crystal X-ray structures became available. It is still widely applied. A recent example is the analysis of "internuclear exciton coupling" in polynuclear complexes.[21] However, these model theoretical approaches have been cumbersome and/or restricted to certain types of excitations and/or did not deliver accurate results without imposing knowledge derived from experiment onto the calculations. Until quite recently,[22−24] no accurate first-principles theoretical calculations of complete (i.e., over the full experimentally known energy range) CD spectra had been carried out for chiral metal complexes. A preliminary calculated DFT-based CD spectrum of $[Ru(bipy)_3]^{2+}$ was presented in Figure 7 of ref 8 but no details of the method were given. To our knowledge the spectrum was never published elsewhere. The available first-principles studies have focused on organic molecules. See, e.g., refs 25−29 for some recent developments and applications. Because many of the best performing ab initio methods are out of range for large molecules, time-dependent density functional theory (TD-DFT), which combines computational efficiency with often quite reliable accuracy, has been used in the cited studies. In ref 24, Diedrich and Grimme also compared TD-DFT results to those obtained by a coupled-cluster (CC2) and two multireference methods (MRMP2 and DFT/MRCI) for a series of molecules including a tricarbonyl−pentadienal−iron complex. For the transition metal complex, CC2 was not applicable and perturbative methods were also found to be somewhat problematic. The TD-DFT results appeared to be sensitive to the functional used. An acceptable agreement of the low-energy part of the CD spectra with experiment could be obtained with the B3-LYP functional. TD-DFT was previously found to well reproduce excitation spectra of a number of chiral Ru complexes,[30] but no CD computations were carried out. For a recent overview of TD-DFT applied to calculate excitation energies of transition metal systems see ref 31.

The CD spectra of various Co(III) complexes as well as $[Rh(en)_3]^{3+}$ were calculated with TD-DFT and analyzed by Autschbach et al. in ref 22. Solvent effects were shown to improve significantly the computed excitation energies for charge-transfer bands for some of the complexes with charge +3, but to have only a small influence on those for less-charged systems. Using

* To whom correspondence should be addressed. E-mail: jochena@buffalo.edu.
‡ University at Buffalo.
† Present address: Lehrstuhl für Theoretische Chemie, Universität Bonn, Wegelerstrasse 12, D-53115 Bonn, Germany.
§ Universität Erlangen.

10.1021/jp0444363 CCC: $30.25
Published on Web 05/11/2005

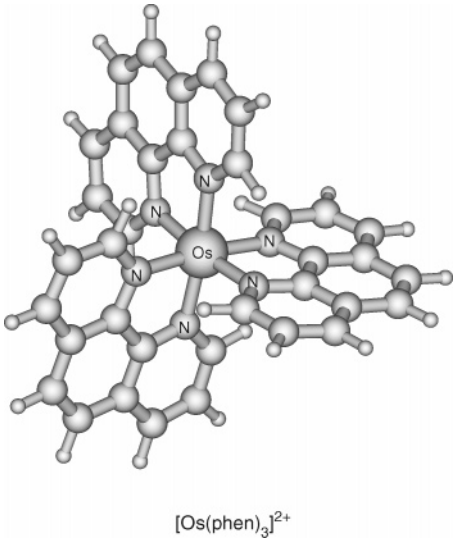

Figure 1. Optimized structure of the complex Λ-[Os(phen)$_3$]$^{2+}$ as an example of the structure of the Λ-[M(phen)$_3$]$^{2+}$ systems studied here.

similar TD-DFT computations, the same authors have later extended the analysis of the optical activity in the d-to-d as well as the ligand-to-metal charge-transfer (LMCT) transition regions to a larger series of tris-bidentate Co(III) and Rh(III) complexes.[23,32] It was shown how configurational distortions of the ligands from a perfect octahedron are responsible for the sign and energetic ordering of the various CD bands, and how the TD-DFT approach can be used to validate or disprove various older crystal-field theory based approaches. In all these studies, the agreement with experiment was found to be semiquantitative at best. Differences of about a factor of 2 between calculated CD intensities and the experimental values were found to be typical for weak CD bands when using an empirical recipe for the line width originally employed by Brown at al.[33] in 1971. The agreement was often better for more intense CT transitions. Of course, the simulated CD intensity depends on the chosen line width, which in reality may or may not vary significantly over the studied frequency range. However, cases where experimental rotatory strengths are available in the literature indicated that the calculated rotatory strengths might indeed be somewhat too large for transitions involving metal d-orbitals.

It was argued in ref 22 that deficiencies of the density functionals might be responsible for sometimes sizable errors found for the calculated excitation energies. On the other hand, the shape of the simulated spectra agreed very well with the experimental ones, which suggests that the main sources of error were rather the calculated excitation energies, not the rotatory strengths. A (very limited) comparison between Co(III) and Rh(III) indicated that nonhybrid density functionals might perform quite accurately for systems with heavier metals, and that in addition to known problems, for instance with the adiabatic exchange-correlation (XC) kernel to describe charge-transfer excitations,[34] the deficiencies in the functionals are likely to cause errors for d-to-d transitions involving 3d metals.

In this work, we apply TD-DFT to expand the still very limited experience with the calculation—and ultimately the prediction—of CD spectra for chiral metal complexes over the whole experimentally accessible energy range (here between 15 and 45 × 10^3 cm^{-1}). The question of whether TD-DFT performs better for CD spectra of complexes of heavier metals than for 3d metals has not been sufficiently investigated. Thus, we have decided to address this issue in the present work. Further, we investigate the influence of relativistic corrections on the CD spectra of 5d metal complexes, as well as basis set, geometrical, and solvent effects. The compounds studied here are [M(phen)$_3$]$^{2+}$ where M is either Os, Ru, or Fe, and phen = 1,10-phenanthroline. This series of compounds is well-suited for the purpose of this study because the CD spectra in the UV−vis energy range afford metal-to-metal (MM) d-to-d transitions, metal-to-ligand (MLCT) charge transfer, exciton coupling CD for the unsaturated ligand's $\pi-\pi^*$ transitions, and increasing relativistic effects in the metals' valence shells along the series Fe, Ru, Os. Current research interest in excited states of compounds of this type, in particular with Ru, is significant,[35−39] with proposed applications in many fields of chemistry[8] but also materials science,[40−43] biology,[44] biochemistry,[45] and medicine.[39,45−48] The present work is restricted to vertical singlet excitations. Apart from the study of the circular dichroism of [M(phen)$_3$]$^{2+}$ itself, though the interest for technological applications is not only in excited singlet but also triplet states of such metal systems, our findings might assist other researchers by defining suitable computational models for computations of excitation energies and transition moments. CD spectra are more difficult to reproduce qualitatively correctly than UV−vis spectra because of the varying signs of the rotatory strengths. Deficiencies in the computational models are thus more likely to lead to disagreement of simulated and experimental spectra.

The paper is organized as follows: In section 2 we outline the computational details. Section 3 is devoted to the presentation and discussion of the computational results and the comparison with experimental data. We finish in Section 4 with some concluding remarks.

2. Computational Details

Scalar relativistic computations of singlet excitation energies and rotatory strengths, based on the zeroth-order regular approximation (ZORA) Hamiltonian,[49,50] were carried out with the 2004 version of the Amsterdam Density Functional (ADF) program package.[51−53] The CD functionality by Autschbach et al.[26,54,55] is an extension of the TD-DFT module in ADF previously developed by van Gisbergen, Baerends, et al.[56−58] Typically, the 50 lowest excitations were calculated (in some cases 70) in order to cover the energy range of the experiments. Rotatory strengths are reported here based on the dipole-length expression. It has been shown previously[22] that the dipole-velocity expression yields very similar simulated CD spectra for metal complexes with the basis sets that we applied here. When calculated from the dipole-velocity representation, the rotatory strengths are gauge-origin independent. Though we did not employ a gauge-including atomic orbital basis[59] (GIAO), the similarity between the simulated spectra in dipole-length and dipole-velocity form in the common-gauge approach indicates that the results are likely not to change in a qualitative sense when switching to a GIAO basis (i.e., the overall appearance of the CD spectra will remain the same). It has previously been argued that "global" mixed electric−magnetic response properties, unlike chemical shifts, can be meaningfully calculated within a common-gauge origin approach if basis sets are employed that are adequate to achieve good agreement between theory and experiment.[55,60]

From the computed singlet excitation energies and rotatory strengths, CD spectra were simulated as previously described in refs 22 and 26 in order to allow for an easier comparison with experimental data. The software used to simulate the spectra is available from our group's WWW server.[61] The CD spectra were calculated for the optical antipodes of the

TABLE 1: Major Contributions (in %) from Occupied−Unoccupied Orbital Pairs to the Transition Dipole Moments of Some Excitations of $[Os(phen)_3]^{2+}$ (TZ2P/TZP Basis, BP Functional)[a]

				major contribution to transition dipole moment		
no.	sym	ΔE/ 10^3 cm^{-1}	R/ 10^{-40} cgs	MO → MO	%	assignment
A	$^1A_2$	14.3	33.87	$19a_1 \rightarrow 18a_2$	99	Os → π^* phen
B	^1E	16.9	48.22	$35e \rightarrow 18a_2$	45	Os → π^* phen
				$19a_1 \rightarrow 37e$	27	
				$19a_1 \rightarrow 36e$	25	
C	^1E	17.4	45.16	$19a_1 \rightarrow 37e$	58	Os → π^* phen
				$35e \rightarrow 18a_2$	23	
				$35e \rightarrow 36e$	15	
D	^1E	20.6	−57.94	$35e \rightarrow 36e$	64	Os → π^* phen
				$35e \rightarrow 18a_2$	10	
				$35e \rightarrow 37e$	11	
E	^1E	35.6	801.23	$18a_1 \rightarrow 36e$	17	π phen → π^* phen
				$34e \rightarrow 19a_2$	13	
				$33e \rightarrow 36e$	12	
F	$^1A_2$	36.5	−1315.9	$33e \rightarrow 36e$	26	π phen → π^* phen
				$18a_1 \rightarrow 18a_2$	12	
				$34e \rightarrow 38e$	10	
G	^1E	38.9	82.52	$32e \rightarrow 18a_2$	42	π phen → π^* phen
				$33e \rightarrow 19a_2$	18	
H	$^1A_2$	39.2	−264.17	$18a_1 \rightarrow 19a_2$	50	π phen → π^* phen
				$33e \rightarrow 38e$	25	
				$34e \rightarrow 38e$	11	
I	$^1A_2$	42.8	−145.58	$35e \rightarrow 41e$	38	π phen → π^* phen
				$31e \rightarrow 37e$	32	and Os → π^* phen

[a] See the MO diagram in Figure 9 for orbital energy levels and Figure 2 for labels A, B, C, etc. of the excitations.

experimentally studied species (Λ configurations) and have thus been inverted. We have obtained overall reasonable agreement with experiment when choosing a Gaussian line width parameter σ of 0.13 eV for all simulated spectra. Numerical data for the experimental spectra were extracted from graphical material accessible in the literature[17] with the help of the g3data software.[62] A frozen core triple-ζ doubly polarized TZ2P Slater basis set was employed for the metal atoms in most of the TD-DFT calculations, whereas the TZP basis set was used for N, C, and H. Inner shells up to 4f, 3d, and 2p for Os, Ru, and Fe, respectively, were kept as frozen cores in the calculations (60, 28, and 18 frozen core electrons, respectively). The 1s shell was kept frozen for C and N. Test calculations on $[Co(en)_3]^{3+}$ have previously shown that while the values of the rotatory strengths and excitation energies change somewhat, there are no significant modifications in the simulated CD spectra when including additional polarization functions on the metal. The TZP on the ligands and the TZ2P basis sets on the metal appear to offer enough flexibility.[22] This has further been confirmed by additional test calculations on $[Os(phen)_3]^{2+}$ for the present work. Because of the size of the complexes and the fact that valence excitations determine the spectra in the UV−vis range, diffuse functions on the ligands are not expected to significantly improve the spectra.

In addition to calculations with ADF, we have also carried out CD spectra computations with the TURBOMOLE code[63] employing the CD functionality by Furche et al.[25,64,65] The TZVP basis from the TURBOMOLE basis set library has been used in all calculations, along with a default 28 and 60 electron relativistic effective core potential[66] (ECP) for Ru and Os, respectively. Unless explicitly noted otherwise, results presented in the graphics, Table 1, and the Supporting Information are based on ADF calculations.

Different density functionals were applied, as discussed in the next section. In all computations with ADF, as in previous

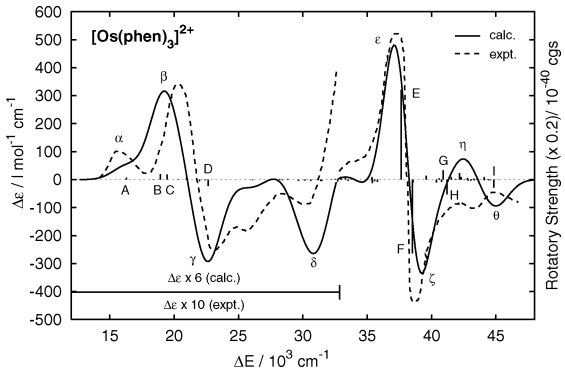

Figure 2. Experimental and simulated CD spectra for Λ-$[Os(phen)_3]^{2+}$. Calculated excitation energies and rotatory strengths are indicated by line spectra. Rotatory strengths were scaled by a factor of 0.2. Calculated excitations are blue shifted by 2.0×10^3 cm^{-1}. The low-energy part of the experimental (simulated) CD spectrum up to 33×10^3 cm^{-1} is magnified by a factor of 10 (6). The BP functional for the exchange-correlation potential, the ALDA kernel, TZ2P (metal)/TZP (ligands) basis sets, and a BP optimized geoemtry were used.

work,[22] the adiabatic LDA (ALDA) kernel has been used for the frequency-dependent linear response of the molecular potential. In the TURBOMOLE computations, the respective adiabatic exchange-correlation (XC) kernel consistent with the functional used for the exchange-correlation potential in the ground state calculation has been employed (either adiabatic GGA (AGGA) or adiabatic hybrid kernels). We have applied the Vosko−Wilk−Nusair (VWN)[67] local density approximation (LDA) combined with Becke−Perdew (BP),[68,69] Perdew−Wang (PW91)[70] or the revised Perdew−Burke−Ernzerhof (revPBE)[71−74] generalized gradient approximations (GGAs), and the B3-LYP hybrid functional. Further, the asymptotically correct Kohn−Sham potential "statistical average of orbital potentials" (SAOP),[75] and an effective exact-exchange potential, the Localized Hartree−Fock (LHF) potential[76,77] (cf. also refs 78 and 79), have been employed along with the ALDA and adiabatic BP (ABP) XC kernel. Both potentials have recently been successfully applied to various response properties.

Most TD-DFT calculations were carried out based on geometries optimized with ADF, using the BP functional and the TZ2P basis set with frozen core (details are available in the Supporting Information). Some additional calculations for Λ-$[Fe(phen)_3]^{2+}$ were performed based on a B3-LYP/TZVP optimized geometry. Full D_3 symmetry was employed in all calculations. For each excitation λ, the composition of the solution vector $\mathbf{F}_\lambda$ of the TDDFT eigenvalue problem from which the transition dipole moments are computed,[25,26,54] in terms of contributions from pairs of occupied and virtual MOs allows one a convenient and intuitive analysis of the results in terms of "excitations" from occupied to virtual Kohn−Sham orbitals. The energy gaps between occupied and virtual orbitals serve as a zeroth order estimate for the excitation energies.[80]

Graphical representations of molecular orbitals were prepared with the MOLEKEL program.[81,82]

3. Results and Discussion

3.1. General Assessment and Comparison with Experiment. In Figures 2, 3, and 4, the calculated excitation energies and rotatory strengths for the three complexes obtained with the BP nonhybrid functional for the exchange-correlation potential and the ALDA kernel are shown in the form of a "bar spectrum". Simulated CD spectra ($\Delta\epsilon$) are compared to the experimental spectra[17] in the same graphics. We have chosen Λ-$[Os(phen)_3]^{2+}$ as our benchmark system to study the influence

of various functionals, relativistic effects, solvent effects, and the basis set. We will present a more detailed analysis in Section 3.7 but mention already that the (magnified) low-energy parts of the spectra are dominated by MLCT excitations, whereas the most intense pair of CD bands is in all cases due to ligand $\pi \rightarrow \pi^*$ exciton transitions. The metal d-to-d transitions are weak and do not contribute much to the main CD bands.

For the complexes Λ-[Ru(phen)$_3$]$^{2+}$ and Λ-[Os(phen)$_3$]$^{2+}$, the agreement with experiment is very good—in fact much better than with any of the CD spectra of transition metal complexes previously presented in the literature. All main features in the experimental spectra are well reproduced by the computations, both for transitions formally involving only the ligands as well as for those where the metal participates to a large extent. For Λ-[Fe(phen)$_3$]$^{2+}$, however, the signs of the three energetically lowest CD bands are not correctly reproduced, indicating some difficulties with the 3d metal. TD-DFT with nonhybrid functionals has been applied successfully to model the electronic excitations of many organic ligands in organometallic systems.[31] Thus, when beginning with this study we did not expect particular difficulties to model the $\pi \rightarrow \pi^*$ region of the CD spectra of the complexes considered here. The comparison of our results with experiment for all three complexes indeed supports this view.

Nonhybrid functionals were previously reported to have difficulties, for example, to reproduce chemical shifts of 3d metals accurately, in particular for iron chemical shifts,[83] whereas chemical shifts of 4d and 5d metals are well (often better) described at the nonhybrid DFT level.[84] Because the rotatory strength occurs from considering a mixed electric−magnetic perturbation of the molecule it might be expected that problematic cases in NMR calculations also pose problems in calculations of circular dichroism. When comparing the CD spectra of the three complexes with experiment it is seen that those parts of the CD spectrum of Λ-[Fe(phen)$_3$]$^{2+}$ are not reproduced qualitatively correctly where metal 3d orbitals play a major role (see analysis for Λ-[Os(phen)$_3$]$^{2+}$ below). Thus, our finding of good agreement with experiment for Ru and Os but not Fe is likely not just a mere coincidence with similar experiences in computations of metal chemical shifts for 3d, 4d, and 5d metals. However, we will show in a subsequent section that an agreement or disagreement with the experimental solution spectrum of Λ-[Fe(phen)$_3$]$^{2+}$ depends rather strongly on the optimized geometry, and that unfortunately the B3-LYP hybrid functional does not perform better for all geometries than, for instance, the BP functional.

The overestimation of the rotatory strength for the low-intensity CD range up to about 32×10^3 cm^{-1} appears to be typical. As already mentioned, we have observed this also in previous work[22] when assuming line widths that represent the CD intensity of the CT excitations reasonably well. We have applied a global blue shift of 2×10^3 cm^{-1} for Λ-[Os(phen)$_3$]$^{2+}$ in order for the strongest CD bands to coincide with the experimental ones. We believe that this shift rather corrects systematic errors due to approximations in the exchange-correlation potentials rather than unspecific solvent effects since we have modeled solvent effects to some extent (see below) and found only minor changes. To be consistent, the same global shift has been applied to the other two complexes for calculations that use the same basis sets and functionals (Figures 3 and 4). This leads to slightly less good agreement with the experimental position of the most intense CD bands for the Ru and Fe complex. However, it should be pointed out again that the energies of the CD bands in all parts of the spectra agree

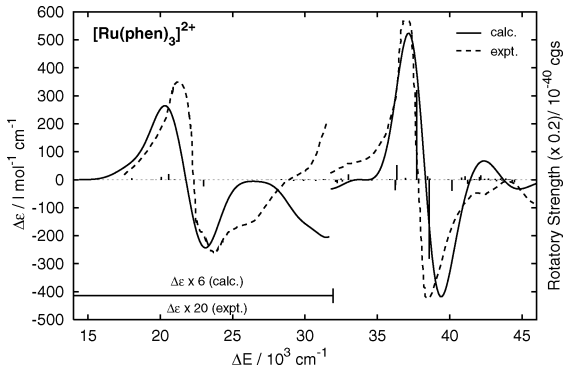

Figure 3. Experimental and simulated CD spectra for Λ-[Ru(phen)$_3$]$^{2+}$. See also the caption for Figure 2.

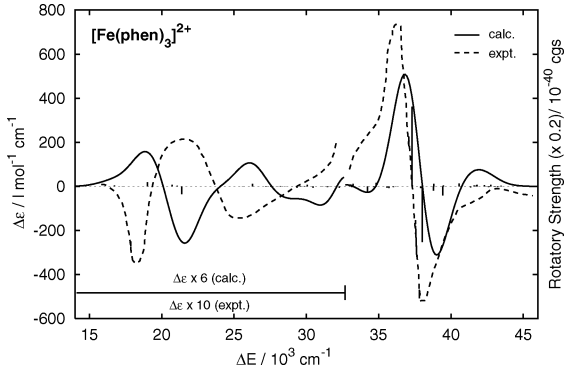

Figure 4. Experimental and simulated CD spectra for Λ-[Fe(phen)$_3$]$^{2+}$. See also the caption for Figure 2.

much better with experiment than in our previous studies on Co(III) complexes where in particular the d-to-d transitions were overestimated in energy by up to 1 eV (8×10^3 cm^{-1}).

One reason the experimental spectra for Os and Ru are particularly well reproduced by the computations here could be that d-to-d transitions do not contribute much to the CD bands in the phen$_3$ complexes. However, as already mentioned for 4d and 5d metals, nonhybrid functionals might be expected to yield more accurate excitation energies of transitions involving metal d-orbitals than for the 3d metal Fe. This viewpoint is also supported by a comparison of CD spectra of Co(III) and Rh(III) in ref 22 where the d-to-d excitations are the only contributors to the low-energy CD bands. The results for Rh(III) agreed much better with experiment. On the other hand, the nature of the ligand also plays an important role. For Co(acac)$_3$, the only Co complex with unsaturated ligands among those that were studied in ref 22, we have in fact obtained by far the best agreement with experiment, similar to what is seen here for the tris-phenanthroline complexes of Ru and Os.

An important purpose of CD spectra calculations is to aid experimentalists in the assignment of the absolute configuration of new compounds.[85] It is clear from the present results that for the 4d and 5d metal complex the accuracy of (fast) nonhybrid TD-DFT is good enough to assign the absolute configuration of the complex, and the individual CD bands, with high confidence (if we did not know the absolute configuration). For the Fe complex, on the other hand, the situation is not so clear. From the knowledge of the nature of the strong $\pi \rightarrow \pi^*$ CD bands it would still be possible to assign the absolute configuration, but the low-energy part of the spectrum almost appears as one calculated for the optical antipode. One reason the Λ-[Fe(phen)$_3$]$^{2+}$ spectrum appears particularly incorrect in the low-energy region is the applied shift. For the Fe complex, no or even a slight red shift would yield better agreement with

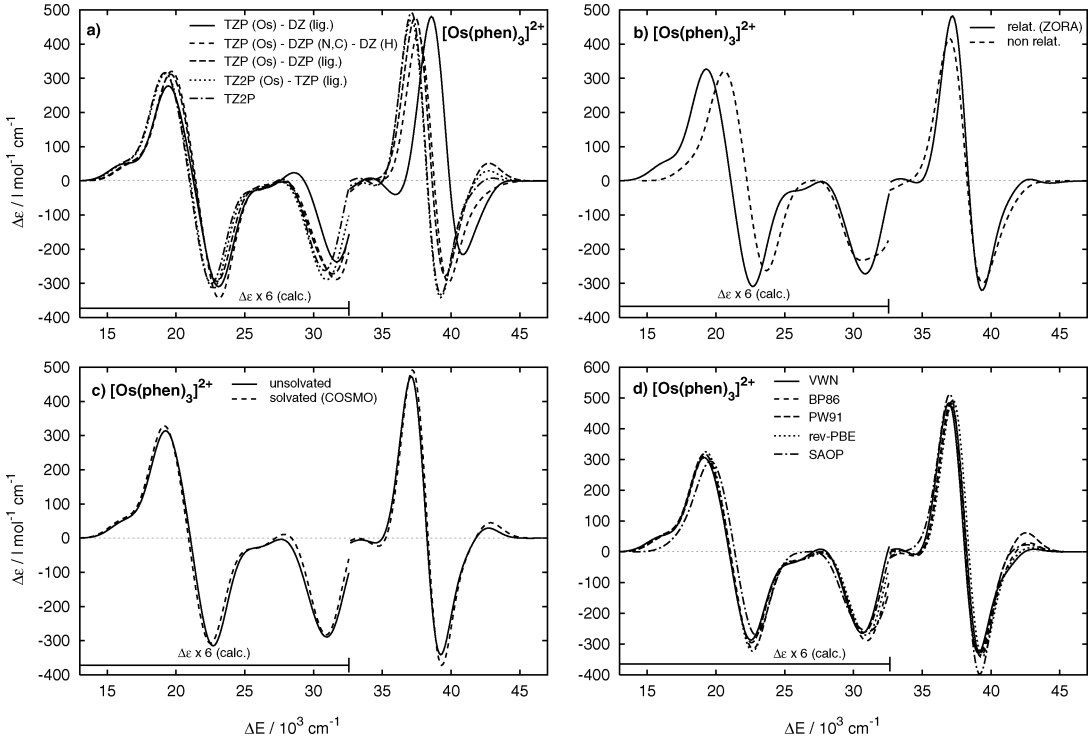

Figure 5. Simulated CD spectra for Λ-$[Os(phen)_3]^{2+}$: (a) for different basis sets, (b) with or without relativistic effects, (c) with or without the inclusion of the solvation (COSMO model) in the ground-state calculations, and (d) for different density functionals for the exchange-correlation potential. In all cases ALDA kernels and BP optimized geometries were used. Calculated excitations are blue shifted by 2.0×10^3 cm^{-1}. The intensity of the low-energy part (below 32.6×10^3 cm^{-1}) has been scaled by a factor of 6. BP exchange-correlation potential for panels a−c, TZ2P/TZP basis for panels c and d, and TZP basis for panel b due to the lack of a nonrelativistic TZ2P basis for Os.

experiment in the $\pi \rightarrow \pi^*$ region. However, a red shift would then predict the presence of a positive CD band below 15×10^3 cm^{-1}, which is not visible in the experiment. We will analyze in a later section what the sources of errors for the Fe complex could be. Our conclusions will be supported by results from calculations employing the B3-LYP hybrid functional for potential and kernel as well as results from calculations with the LHF potential.

3.2. Basis Set Effects. The computed CD spectra of Λ-$[Os(phen)_3]^{2+}$ for various basis sets are shown in Figure 5a. Though small differences remain between all the simulated CD spectra, it can be seen that the largest effects result from adding polarization functions on the "heavy" (C, N) atoms of the ligands (DZ versus DZP). Because the CD spectrum is dominated by valence excitations in a rather large molecule we do not expect substantial improvement by adding diffuse functions to the basis. Test calculations with additional polarization functions on the metal have confirmed previous findings[22] that the TZP or TZ2P basis is sufficiently flexible for the metal because it can benefit from added flexibility provided by the ligand's basis functions.

Regarding comparisons of the basis sets applied with ADF and TURBOMOLE, we should note that when using the same functional (BP) for the exchange-correlation potential and the same kernel (ALDA) the simulated spectra obtained with TURBOMOLE and the TZVP basis agree very well with those obtained with ADF and the TZ2P/TZP basis (despite small differences in the excitation energies). They are therefore not shown. This also demonstrates that, as expected, the pseudopotential and the scalar ZORA approach lead to very similar relativistic valence orbitals for Ru and Os. For the Fe complex, the differences are somewhat larger but not particularly significant when compared with the differences between both calculations and experiment. For instance, the calculated CD intensities in the low-energy range calculated with the TZVP basis are twice as large as those calculated with the TZ2P/TZP basis and thus overestimate the experimental intensities even more. However, the overall shape of the simulated spectra is the same. Differences in the rotatory strengths occur mainly for the MLCT excitations where the use of the LDA XC kernel in the ADF calculations might play a role.

3.3. Density Functional Issues. In Figure 5d, we present a comparison of various XC potentials for calculating the CD spectrum of $[Os(phen)_3]^{2+}$. (Spectra a−c in Figure 5 are based on computations with the BP exchange-correlation potential and the ALDA kernel.) It can be seen that the use of other gradient-corrected functionals for the exchange-correlation potential, such as PW91 or revPBE, does not improve—or even significantly change—the calculated spectra. Also, the use of the asymptotically corrected Kohn−Sham potential SAOP does not lead to any significant improvement. This is understandable because the accessible range of the CD spectra is based on valence excitations whereas SAOP, though affording features other than just the asymptotic correction, differs from the GGAs mainly in the shape and energies of rather diffuse virtual orbitals that should not have a strong influence on the CD spectrum of Λ-$[Os(phen)_3]^{2+}$. Likewise, for Λ-$[Fe(phen)_3]^{2+}$ the SAOP potential offers no improvement over the BP potential. Our findings here are in line with previous work,[22] where we also found that for Co complexes CD spectra obtained with different nonhybrid density functionals (VWN, BP, SAOP) all exhibited similar errors when based on the same geometry.

Rosa et al.[31] have recently pointed out that the performance of hybrid functionals for excitation energies of 3d metal complexes is all but consistent. However, considering the good performance of B3-LYP for Fe chemical shifts that was reported in the literature[83] we might expect some improvement for the Λ-$[Fe(phen)_3]^{2+}$ CD spectrum. In Figure 6 we display results for Λ-$[Fe(phen)_3]^{2+}$ obtained with the B3-LYP functional for

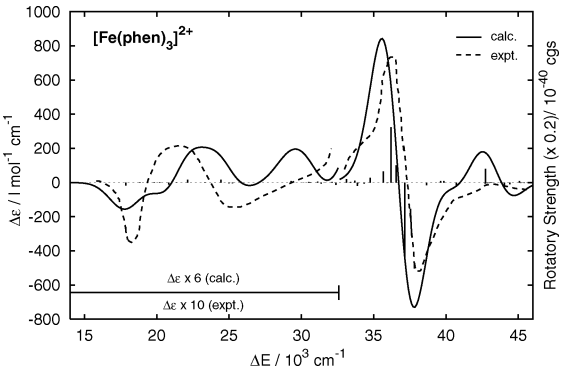

Figure 6. Experimental and simulated CD spectra for [Fe(phen)$_3$]$^{2+}$ using the B3-LYP functional for the exchange-correlation potential and kernel (TURBOMOLE, TZVP basis), and a BP optimized geometry. Calculated excitation energies and rotatory strengths are indicated by line spectra. Calculated excitations are red shifted by 2.0×10^3 cm^{-1}. CD intensity and rotatory strengths have been scaled as indicated in the figure.

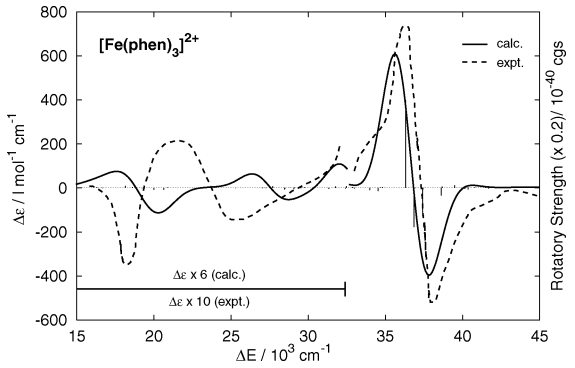

Figure 7. Experimental and simulated CD spectra for [Fe(phen)$_3$]$^{2+}$ using the LHF potential, ABP kernel, and BP geometry. See also the caption for Figure 6. Calculated excitations are not shifted.

the exchange-correlation potential and kernel at the optimized BP geometry. The simulated spectrum agrees better with the experimental one, though the agreement is not as good as what has been obtained for the other two complexes. It should be noted that a global red shift of 2×10^3 cm^{-1} has been applied to achieve an overall reasonable matching of the CD band's maxima.

In contrast to Λ-[Fe(phen)$_3$]$^{2+}$, the simulated CD spectra based on the BP/ALDA calculations for the 4d and 5d complex are very similar to their B3-LYP counterparts (and therefore not shown here). This result suggests that it is indeed the presence of the 3d metal that causes the differences. Moreover, also the Λ-[Fe(phen)$_3$]$^{2+}$ *experimental* spectrum is qualitatively different from the other two in the low-energy region. Interestingly, the calculated GGA/ALDA spectra for all 3 complexes are qualitatively equivalent. This seems to suggest that important features which distinguish Fe from the other group 8 elements are not contained in the approximate treatment of the electronic structure at the GGA/ALDA level. The fact that the spectra for Λ-[Fe(phen)$_3$]$^{2+}$ are virtually identical when calculated with ADF using the BP potential and the ALDA kernel and with TURBOMOLE using the BP potential and the consistent BP kernel (spectrum not shown here) further proves that missing GGA corrections in the exchange-correlation kernel do not make the main difference here.

To further investigate this issue, we have carried out a TDDFT calculation employing the ABP GGA kernel on top of a B3-LYP ground state calculation. We do not assign physical significance to the results of this calculation and consequently do not tabulate them. However, this calculation allows us to obtain a rough estimate of whether the exact exchange contribution in the hybrid-GGA kernel is mostly correcting the difference between the nonhybrid and hybrid DFT orbital energies when evaluating the excitation energies, or whether there are more complicated (and important) contributions. When simulating a CD spectrum from this calculation, not surprisingly a large red shift of 1.25 eV (10.1×10^3 cm^{-1}) compared to the red shift of 2.0×10^3 cm^{-1} of the pure (potential and kernel) B3-LYP calculation needs to be applied in order to align it with the experimental CD bands. After shifting, however, the spectrum is rather similar to the GGA CD spectrum and does not agree with the experiment in the low-energy range. This means that B3-LYP both shifts back the orbital energy differences and takes influence on the low-energy part of the spectrum.

The first, lowest energy, CD band of Λ-[Fe(phen)$_3$]$^{2+}$ in the B3-LYP spectrum is due to the lowest energy excitation with a sizable rotatory strength of -86×10^{-40} cgs units. This excitation shows a strong mixing of occupied-to-virtual orbital pair contributions (five, with weights of 53%, 27%, 8%, 2%, and 2% in the square of the transition vector $\mathbf{F}_\lambda$). The occupied-virtual orbital energy differences for the strongest contributions (nos. 1 and 2) are more than 2 eV higher than the HOMO-LUMO gap $28a_1 \rightarrow 50e$, which corresponds to the third-largest contribution with only 8%. This indicates a strong influence from the XC kernel. The symmetry of the lowest two transitions in the pure B3-LYP calculation is E/A$_2$ (in ascending energy order) with CD signs $-/+$. Both the BP potential with the ALDA kernel as well as the B3-LYP potential with the ABP kernel, on the other hand, yield A$_2$/E with signs $+/-$. The excitations in both cases are composed from either a single occ-virt MO pair contribution or a mixing of such contributions with very similar orbital energy differences, due to symmetry. None of them exhibits any strong contributions from occupied-virtual orbital pairs with much larger energy gaps, as is the case when the B3-LYP kernel is used, which would shift the E-transition with negative rotatory strength below the lowest A$_2$ transition with positive rotatory strength. Along with the discussion from the previous paragraph, we interpret these results such that the low-energy part of the Λ-[Fe(phen)$_3$]$^{2+}$ CD spectrum is caused by rather subtle features in the response of the electronic structure that are described differently by an ALDA or AGGA kernel compared to an adiabatic hybrid-XC kernel.

An important shortcoming of LDA as well as GGA exchange-correlation potentials is that they do not sufficiently cancel the self-interactions of electrons contained in the Coulomb potential. The most pronounced effect of this self-interaction is the wrong asymptotic behavior of LDA and GGA potentials. However, the self-interaction affects the LDA and GGA potentials in all regions of space, not only the asymptotic region. To analyze the effect of Coulomb self-interactions in the exchange-correlation potentials on the calculated CD spectra, a calculation with a self-interaction free Kohn−Sham potential had to be carried out. To this end, we have performed a computation on Λ-[Fe(phen)$_3$]$^{2+}$ employing the LHF potential developed by Della Sala and Görling[76,77] (cf. also refs 78 and 79) together with the ABP kernel for reasons of consistency with the other BP calculations with TURBOMOLE. The LHF potential is an effective exact-exchange Kohn−Sham potential and as such cancels the self-interactions of the Coulomb potential. The resulting CD spectrum is shown in Figure 7 in comparison with experiment. It can be seen that the $\pi \rightarrow \pi^*$ region of the spectrum agrees very well with the spectrum obtained with the

BP potential and the ALDA kernel shown in Figure 4. However, the BP/ALDA spectrum had to be blue shifted by 2×10^3 cm^{-1} to achieve good agreement with experimental data. For the LHF/ABP spectrum a shift of only 0.5×10^3 cm^{-1} would be required for perfect agreement of the strongest CD bands, which is clearly an advantage at this point. We have noted that the results with the LHF potential show a slight dependence on which adiabatic nonhybrid kernel is used. For instance, using the ALDA kernel instead of ABP shifts the $\pi \rightarrow \pi^*$ CD bands by 0.5×10^3 cm^{-1}. However, there is little effect on the simulated CD spectrum otherwise. Results obtained with the adiabatic Becke88 exchange-only kernel are virtually indistinguishable from the ones obtained with the ABP kernel. More important here is that the low-energy range of the LHF/ALDA and LHF/ABP CD spectra is also very similar to that of the shifted BP/ALDA spectrum shown in Figure 4, with an energetic ordering of A_2/E and signs +/− for the lowest two excitations that do not reproduce the experiment qualitatively. Tentatively, therefore, though the analysis is somewhat limited by the size and complexity of the systems, our results suggest that the apparent failure of the nonhybrid functionals for the 3d metal at the BP geometry is due either to a superior treatment of electron correlation by the hybrid functional or to self-interaction errors in the ALDA or AGGA XC kernels, but probably not due to self-interaction errors of the nonhybrid exchange-correlation potential employed in the ground-state calculation. The calculation employing the B3-LYP functional along with an AGGA kernel indicates that the differences in the B3-LYP and AGGA exchange-correlation *kernel* might be more important for the present case.

3.4. The Influence of the Geometry. Because the CD spectrum is caused by contributions of varying sign, the energetic ordering of the excitations is crucial to obtain a qualitatively, let alone a quantitatively, correct calculated spectrum. Obviously, for Λ-$[Fe(phen)_3]^{2+}$ in particular, small differences in the lowest excitation energies matter. Therefore, the question arises whether small changes in the geometry of the Fe complex might lead to a different performance of the various functionals.

The BP geometry compares very well with available single-crystal X-ray diffraction data.[86,87] For instance, R(Fe−N) = 1.972 Å (calcd) vs 1.978 (exptl, ref 86) or 1.97 (exptl, ref 87), N−Fe−N angle (cis, same phen) = 82.6° (calcd) vs 82.6 (ref 86) or 82.9 (ref 87), N−Fe−N angle (trans, opposite phen) = 175.4° (calcd) vs 175.2 (ref 86) or 176.3 (ref 87). For comparison, the optimized geometry for Λ-$[Fe(phen)_3]^{2+}$ at the B3-LYP/TZVP level yields values of 2.037 Å, 81.3°, and 174.4°, respectively, which do not compare as favorably with the X-ray structure data. On the other hand, there are some uncertainties as to what degree crystal packing compared to solvation affects the structure, which is relevant since we are comparing with solution spectra obtained at room temperature. Nonetheless, the simulated spectra based on the B3-LYP geometry that are displayed in Figure 8 show, in comparison with the BP-geometry spectra in Figures 3, 6, and 7, that the small geometry change between BP and B3-LYP has a profound impact on whether the low-energy range of the CD spectrum agrees qualitatively with experiment or not. In particular, the B3-LYP spectrum obtained at the B3-LYP geometry is not as favorable anymore, whereas the BP spectrum now agrees quite well with experiment, except for the underestimation of the CD intensity in the $\pi \rightarrow \pi^*$ region at the chosen line width of 0.13 eV. The LHF-(ABP) spectrum agrees less well with experiment than the BP one at this geometry, but better than the LHF(ABP) one obtained at the BP geometry.

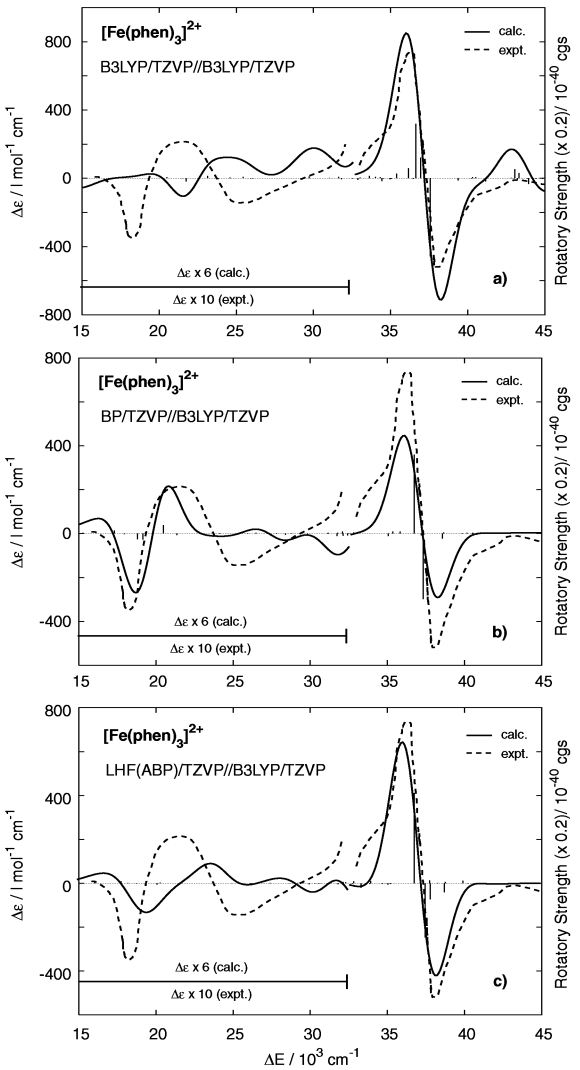

Figure 8. Experimental and simulated CD spectra for $[Fe(phen)_3]^{2+}$ at the B3-LYP optimized geometry: (a) B3-LYP potential and kernel; (b) BP potential and kernel; and (c) LHF potential and ALDA kernel. See also the caption for Figure 7. Calculated excitations are shifted by -2×10^3 cm^{-1} for panel a and $+1 \times 10^3$ cm^{-1} for panel b. No shift was applied for panel c.

Table S3 in the Supporting Information lists the irreducible representations and energies of the highest occupied and lowest unoccupied Kohn−Sham orbitals of Λ-$[Fe(phen)_3]^{2+}$ calculated with different exchange-correlation potentials based on the two geometries optimized (using the BP or B3LYP functional, respectively). In general, it seems difficult to relate the different shapes of the calculated CD spectra to the corresponding electronic structure descriptions. However, it may be worthwhile to note that the low-energy part of the spectra is critically influenced by a transition labeled 7E, which can be projected on a transition from the $28a_1$ occupied orbital to the 53e unoccupied orbital. The energy of the 53e virtual orbital is almost 0.3 eV lower in BP//B3LYP than in BP//BP, while all the other orbital energies differ by usually less than 0.1 eV. The concomitant change in the electronic transition energy may partly be held responsible for the notable differences of the two corresponding spectra.

The pronounced functional- and geometry-dependence of the Λ-$[Fe(phen)_3]^{2+}$ spectrum indicates that though there are likely issues related to deficiencies in the XC kernel, this system is somewhat too sensitive to serve as an easy benchmark test for a functional's performance; i.e., the simultaneous dependence

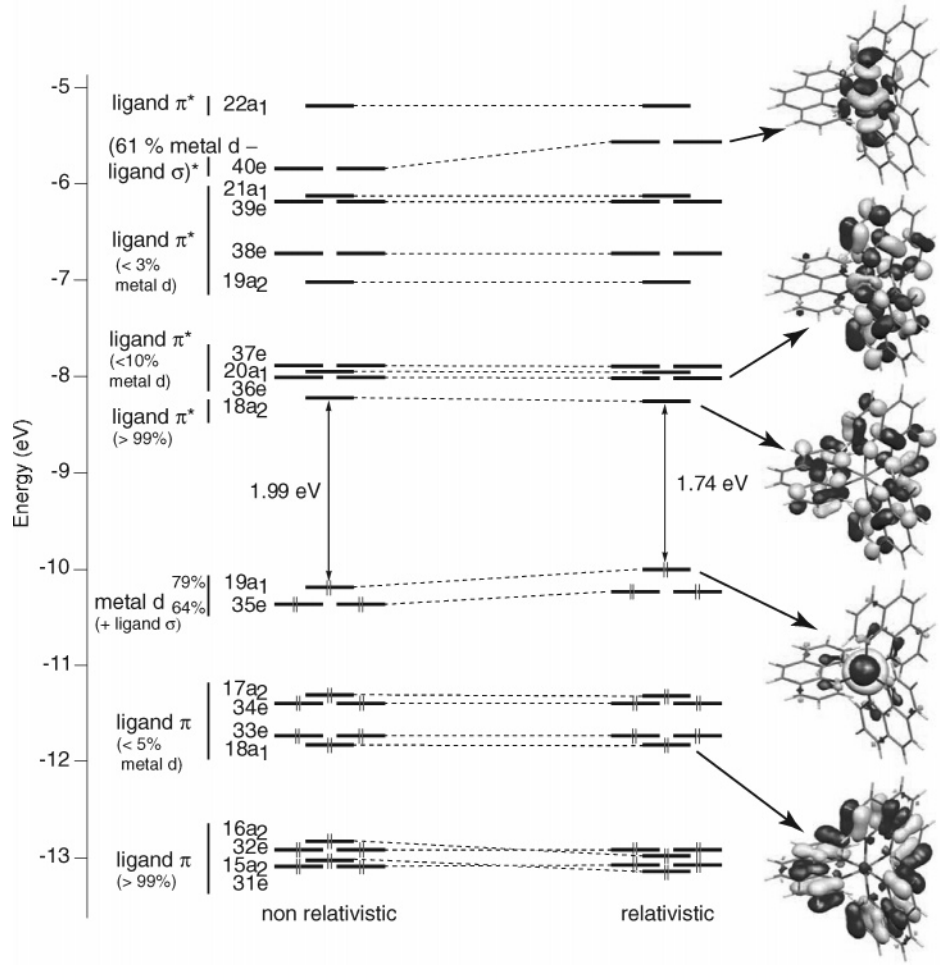

Figure 9. Orbital energy diagrams including and excluding relativistic effects (ZORA, BP functional, TZP basis) for the complex [Os(phen)$_3$]$^{2+}$. The orbital numbering excludes the 30 frozen core orbitals of Os. The orbital diagram for Λ-[Ru(phen)$_3$]$^{2+}$ is almost quantitatively the same as the nonrelativistic one for the Os complex. For the orbital energies of Λ-[Fe(phen)$_3$]$^{2+}$ see Table S3 in the Supporting Information.

of the CD spectrum on the geometric structure obscures the conclusions drawn from a comparison of various functionals at the same geometry. It should be noted that similar conclusions regarding Fe NMR chemical shifts and their geometry and functional dependence were recently drawn.[88] MD simulations including solvent molecules are currently performed by us to elucidate whether the protocol "B3-LYP geometry−BP spectra" is a reasonable pragmatic choice to simulate solution spectra, albeit unsatisfactory from a theoretical consistency viewpoint. With the sensitivity of the spectrum with respect to geometry changes taken into consideration, for instance, the success or nonsuccess of a particular combination of Kohn−Sham potential and kernel with the geometry optimized including solvent effects at the COSMO level would not be convincing without verifying that a dynamical simulation including solvent molecules leads to similar results.

3.5. Relativistic Effects. The influence of relativistic effects on the calculated CD spectrum for [Os(phen)$_3$]$^{2+}$ is demonstrated in Figure 5b by a comparison of the simulated CD spectra with and without relativistic effects included in the computation. Because of the lack of a nonrelativistic TZ2P basis for Os we have used the TZP basis for all atoms in both calculations. The main differences appear in the low-energy region where the CD bands are mainly due to excitations involving metal d-orbitals. These bands are red shifted because of the decrease of the HOMO-LUMO gap corresponding to an expected relativistic indirect destabilization of the occupied metal d-orbitals (HOMO and HOMO-1). This relativistic effect is also clearly visible from a comparison of the molecular orbital diagrams, Figure 9. Other relativistic effects which are seen as a change in the energetic ordering of the lower lying occupied orbitals 31e, 32e, 15a$_2$, and 16a$_2$ as well as the very pronounced shift of 40e (which has a large metal 5d character) are hardly visible in the simulated CD spectrum except for small changes in the maximum intensities because they cause energetic shifts of CD transitions that are weak compared to the dominating $\pi \rightarrow \pi^*$ transitions which are not significantly altered by relativistic effects. This also indicates that an indirect participation of the metal's orbitals in the $\pi \rightarrow \pi^*$ CD is either small or very little influenced by relativity.

3.6. Solvent Effects. In our previous work, ref 22, the influence of the solvent in the calculation of the CD spectra of Co complexes has been investigated by means of the "COnductor-like Screening MOdel" (COSMO)[89,90] applied to the ground state calculations. The solvent was water in all cases but one. It was shown that acceptable agreement of LMCT excitation energies with experimental spectra for some of the highly charged complexes can only be achieved if the solvent is considered in the calculation. For the well-studied "benchmark" complex [Co(en)$_3$]$^{3+}$, the solvent shift of the CT CD bands obtained from such a continuum solvent treatment is modest (about $+2 \times 10^3$ cm^{-1}), but for [Co(tn)$_3$]$^{3+}$, it amounts to almost 7×10^3 cm^{-1}, bringing the calculation into much better agreement with experiment. For less, even +2, charged systems such as the ones calculated here and other +1 and +2 charged systems investigated previously,[22] the simulated spectra

are not strongly altered by the presence of the solvent. These previous findings are corroborated by the present study. See Figure 5c for a comparison of the Λ-$[Os(phen)_3]^{2+}$ spectrum including and excluding solvent effects. A missing contribution in the COSMO solvent treatment as presently implemented is due to the electric polarization of the solvent's electron density. We expect this contribution to be negligible for +3 charged systems and highly polar solvents such as water, and small to negligible for lesser charged systems and the same solvent. A demonstration that the solvent's polarization is negligible for the $[Co(en)_3]^{3+}$ spectrum in aqueous solution is under way in a separate study, based on the discrete reaction field solvent model.[91,92]

3.7. Assignment and Analysis of the Λ-$[Os(phen)_3]^{2+}$ Spectrum. Table 1 lists an analysis of those CD transitions in Λ-$[Os(phen)_3]^{2+}$ that contribute most strongly to the bands in the CD spectrum into contributions from pairs of occupied−unoccupied MOs. The labeling of the transitions, A, B, C, ..., and CD bands, α, β, γ, ..., refers to Figure 2. Starting at the low-energy part of the CD spectrum, it can be seen that bands α, β, and γ, up to about 25×10^3 cm^{-1}, are mainly due to MLCT, i.e., from Os d-orbitals to phenanthroline π^* orbitals. The CD band δ is rather unspecific, with many small contributions of varying character. Bands ϵ, ζ, and θ are of course dominated by the ligands' $\pi \rightarrow \pi^*$ transition, with the very intense circular dichroism of the E/F pair being due to the exciton coupling mechanism. The higher lying excitations have again some MLCT character.

The TD-DFT-based analysis is in agreement with the detailed analysis based on experimental and model theoretical data performed by Mason et al.,[17] in particular regarding the MLCT character of the low-energy CD bands and the nature of the exciton CD band around 37×10^3 cm^{-1}. As predicted by a coupling of the 3 long-axis polarized transition dipole moments in a Λ D_3-symmetric configuration of the complex, the A_2 transition would exhibit a negative Cotton effect, the E transition a positive one (excitations E and F in Table 1). The dissymmetry between the rotatory strengths shows that there is a significant amount of interaction between the ligands. The splitting between the most intense transitions E and F is calculated here as 0.9×10^3 cm^{-1}. An experimental average value quoted by Mason et al.[17] is 1.6×10^3 cm^{-1}. Mason and co-workers have speculated about the amount of the metal's participation in the $\pi \rightarrow \pi^*$ exciton CD, in particular via delocalization of the π system through the metal center, as well as about the amount of ligand interaction. From a model calculation, the metal−ligand interaction was estimated to contribute on the order of 10% to the Davydov splitting. In Table 1, only the largest contributions to the transition dipole moments are listed, which sum up to 42% and 48% of the total values for excitations E and F, respectively. Rather small contributions from many other orbital pairs provide the remaining 58% and 52%, respectively, among those also a number with pronounced metal character. The contributions involving orbitals with a large Os 5d component (mainly the occupied orbitals 19a1 and 35e, see Figure 9) add up to about 8% for transitions E and F, showing that the metal definitely participates in these excitations by the same order of magnitude as predicted by Mason et al. long ago. Less important are contributions from virtual MOs with some Os 5d character (mainly 36e, 20a1, and 37e).

To study these excitations further, we have performed calculations based on the Λ-$[Os(phen)_3]^{2+}$ optimized structure, but excluding the metal. Figure 10 displays the resulting simulated CD spectra for the case that (a) the 3 phen fragments

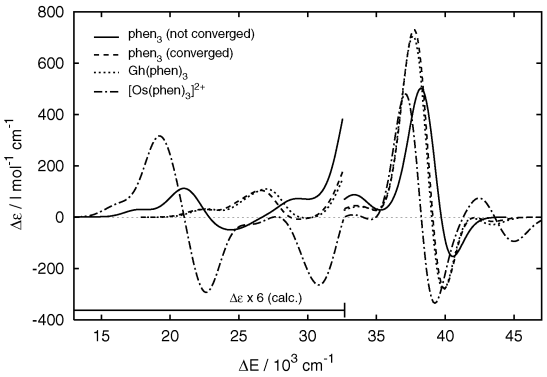

Figure 10. Simulated CD spectra for $[Os(phen)_3]^{2+}$, $Gh(phen)_3$ (with a ghost atom replacing the Os), and the $(phen)_3$ ligand system only. See text for details. BP potential, ALDA kernel, and TZ2P(Os)/TZP-(phen) basis. Calculated excitations are blue shifted by 2.0×10^3 cm^{-1} for consistency with Figure 2.

are placed in the same position as in Λ-$[Os(phen)_3]^{2+}$, with their orbitals kept the same as in free phenanthroline ("unconverged"), (b) same as (a) but after letting the orbitals adapt to the trimer ("converged"), (c) same as (b) but with the basis functions of Os (i.e. an Os Ghost atom) placed in the center ("$Gh(phen)_3$"), and (d) for comparison the simulated spectrum for the full complex Λ-$[Os(phen)_3]^{2+}$. The low-energy part of the CD spectra for cases a−c (up to about 33×10^3 cm^{-1}) is caused by n $\rightarrow \pi^*$ transitions due to the uncoordinated nitrogen lone pairs. Focusing on the $\pi \rightarrow \pi^*$ CD bands only, first we note that there is virtually no difference between cases b and c, i.e., the basis functions of Os as such have no effect. That the metal indeed participates to some extent in the exciton CD in bands ϵ and ζ is also rather obvious from Figure 10 (other than just keeping the ligands together, of course). From the previous analysis of CD band η (excitation no. I in Table 1), it is seen that the metal strongly contributes here, which explains why it is not present for cases a−c. There is also a sizable effect from the relaxation of the ligand orbitals when the three phen units are brought together to form the trimer, mainly visible as a strong increase in the intensity of the exciton CD due both to an increase in the rotatory strengths as well as an increase of 0.2×10^3 cm^{-1} of the splitting between the nearest intense A_2 and E transitions around 37×10^3 cm^{-1}, along with a concomitant red shift of 0.5×10^3 cm^{-1}.

4. Summary

In this paper we have presented a TD-DFT study of the CD spectra of the tris-phenanthroline complexes of Fe, Ru, and Os. The study has taken into account relativistic effects, which were shown to have some impact on the position of the low-energy MLCT bands of Λ-$[Os(phen)_3]^{2+}$. Solvent effects (water) were shown to be rather small for the (+2) charged systems studied here (therefore, only data for Λ-$[Os(phen)_3]^{2+}$ were presented to demonstrate the small solvent influence). It does not appear that the basis set requires diffuse functions or many polarization functions in the metal's basis set. The CD spectra over the experimentally accessible range are caused by valence excitations.

With efficient and parallelized TD-DFT methods as those applied here, it is possible to contribute theoretical support to the assignment of absolute configurations of large metal complexes, and to the study of the electronic excitations of such systems. Compared to previous investigations of CD in Co(III) complexes, the agreement with experiment achieved in this work is very good for the Ru and Os complex, no matter whether

nonhybrid or hybrid functionals were used. The agreement with experiment is comparable to, or even better than, for example, in a pioneering TD-DFT study of various helicenes of ref 25 (where the agreement between theory and experiment was called "excellent"). Most of the CD spectrum of Λ-$[Fe(phen)_3]^{2+}$ is also described well by the computations. The nonhybrid functionals as well as the SAOP and the LHF potentials in conjunction with an ALDA kernel do not reproduce the negative sign of the lowest energy CD band in case the calculations are based on the BP geometry (which agrees well with crystal structure data). At this geometry, usage of the B3-LYP hybrid functional for the exchange-correlation potential and kernel predicts the correct sign of this CD band for Λ-$[Fe(phen)_3]^{2+}$ and leads to acceptable agreement with experiment. However, the situation changes completely when the computations are based on a geometry optimized at the B3-LYP level. Here, the calculation of the CD spectrum based on the BP potential yields good agreement with experiment, whereas the B3-LYP calculation does not reproduce the sign pattern in the low-energy part of the spectrum correctly. Tentatively, some of the problems with the 3d metal can be attributed to deficiencies in the nonhybrid XC kernels. Results obtained with the self-interaction free LHF potential in conjunction with the ALDA and AGGA XC kernels suggest that it is not sufficient to eliminate self-interaction errors in the XC potential alone but not in the kernel simultaneously. However, with such subtle geometry and functional dependencies other yet neglected effects, for instance due to the molecule's vibrations and solvent effects on the geometry, should be considered before trying to devise a pragmatic recipe for which static calculations of vertical excitation energies and rotatory strengths yield good agreement with solution spectra.

In conclusion, considering the results of the present study as well as those of ref 22, the CD spectra of chiral metal complexes with unsaturated ligands are well described at the level of (computationally rather inexpensive) nonhybrid TD-DFT if the metal is from the 4d or 5d row. For a 3d metal complex, correlation and self-interaction errors might play an important role and lead to errors and wrong ordering of energies of transitions involving metal d-orbitals. We were not able to identify a functional that would yield both a geometry and a CD spectrum for Λ-$[Fe(phen)_3]^{2+}$ that agrees well with the experiment.

An analysis of the Λ-$[Os(phen)_3]^{2+}$ CD spectrum has shown that the metal orbitals participate to some extent in the exciton chirality of the phenanthroline's $\pi \rightarrow \pi^*$ transitions. Further, there is a sizable effect from the relaxation of the ligand's orbitals when they form the phen-trimer that coordinates the metal.

Acknowledgment. We acknowledge support from the Center for Computational Research (CCR) at SUNY Buffalo. Some of the computations were performed as part of the Molecular Sciences Computing Facility (MSCF) Grand Challenge project entitled "Reliable Electronic Structure Calculations for Heavy Element Chemistry: Molecules Containing Actinides, Lanthanides, and Transition Metals" at the Environmental Molecular Sciences Laboratory (a national scientific user facility sponsored by the U.S. DOE Office of Biological and Environmental Research) located at Pacific Northwest National Laboratory. J.A. is supported by the National Science Foundation and the Petroleum Research Fund, administered by the American Chemical Society. We are indebted to Dr. Filipp Furche, who provided us with the results of one of the calculations on Λ-$[Fe(phen)_3]^{2+}$.

Supporting Information Available: Optimized structures (Cartesian coordinates) for the complexes $[M(phen)_3]^{2+}$ (M = Os, Ru, and Fe) and $[M(bipy)_3]^{2+}$ (M = Os and Ru) as well as part of the output from the ADF TD-DFT computations with detailed numerical data for the excitation energies and the rotatory strengths; orbital energies for Λ-$[Fe(phen)_3]^{2+}$ obtained with various XC potentials, kernels, and geometries. This material is available free of charge via the Internet at http://pubs.acs.org.

References and Notes

(1) Crabbé, P. *Optical Rotatory Dispersion and Circular Dichroism in Organic Chemistry*; Holden-Day: San Francisco, CA, 1965.

(2) Caldwell, D. J.; Eyring, H. *The theory of optical activity*; Wiley-Interscience: New York, 1971.

(3) Charney, E. *The molecular basis of optical activity*; John Wiley & Sons Ltd.: New York, 1979.

(4) Lightner, D. A.; Gurst, J. E. *Organic Conformational Analysis and Stereochemistry from Circular Dichroism Spectroscopy*; Wiley-VCH: New York, 2000.

(5) Berova, N.; Nakanishi, K.; Woody, R. W., Eds. *Circular Dichroism. Principles and Applications*; VCH: New York, 2000.

(6) Ballhausen, C. J. *Molecular Electronic Structures of Transition Metal Complexes*; McGraw-Hill: London, UK, 1979.

(7) Kuroda, R.; Saito, Y. Circular Dichroism of Inorganic Complexes: Interpretation and Applications. In *Circular Dichroism*: *Principles and Applications*, 2nd ed.; Berova, N., Nakanishi, K., Woody, R. W., Eds.; VCH: New York, 2000.

(8) Ziegler, M.; von Zelewsky, A. *Coord. Chem. Rev.* **1998**, *177*, 257−300.

(9) Condon, E. U. *Rev. Mod. Phys.* **1937**, *9*, 432−457.

(10) Moscowitz, A. *Adv. Chem. Phys.* **1962**, *4*, 67−112.

(11) Oddershede, J. *Adv. Quantum Chem.* **1978**, *11*, 275−352.

(12) Hansen, A. E.; Bouman, T. D. *Adv. Chem. Phys.* **1980**, *44*, 545−644.

(13) Oddershede, J. Propagator methods. In *Ab initio methods in quantum chemistry*; Lawley, K. P., Ed.; John Wiley & Sons: London, UK, 1987; Vol. II.

(14) Koslowski, A.; Sreerame, N.; Woody, R. W. Theoretical Approach to Electronic Optical Activity. In *Circular Dichroism*: *Principles and Applications*, 2nd ed.; Berova, N., Nakanishi, K., Woody, R. W., Eds.; VCH: New York, 2000.

(15) Douglas, B. E.; Saito, Y., Eds. *Stereochemistry of Optically Active Transition Metal Compounds*; ACS Symp. Ser. No. 119; American Chemical Society: Washington, DC, 1980.

(16) Volosov, A.; Woody, R. W. Theoretical approach to natural electronic optical activity. In *Circular Dichroism. Principles and Applications*; Nakanishi, K., Berova, N., Woody, R. W., Eds.; VCH: New York, 1994.

(17) McCaffery, A. J.; Mason, S. F.; Norman, B. J. *J. Chem. Soc. A* **1969**, 1428−1441.

(18) Mason, S. F.; Norman, B. J. *J. Chem. Soc. A* **1969**, 1442−1447.

(19) Král, M.; Moscowitz, A.; Ballhausen, C. J. *Theor. Chim. Acta* **1973**, *30*, 339.

(20) Král, M. *Theor. Chim. Acta* **1979**, *50*, 355−357.

(21) Telfer, S. G.; Tajima, N.; Kuroda, R. *J. Am. Chem. Soc.* **2004**, *126*, 1408−1418.

(22) Autschbach, J.; Jorge, F. E.; Ziegler, T. *Inorg. Chem.* **2003**, *42*, 2867−2877.

(23) Jorge, F. E.; Autschbach, J.; Ziegler, T. *Inorg. Chem.* **2004**, *42*, 8902−8910.

(24) Diedrich, C.; Grimme, S. *J. Phys. Chem. A* **2003**, *107*, 2524−2539.

(25) Furche, F.; Ahlrichs, R.; Wachsmann, C.; Weber, E.; Sobanski, A.; Vögtle, F.; Grimme, S. *J. Am. Chem. Soc.* **2000**, *122*, 1717−1724.

(26) Autschbach, J.; Ziegler, T.; van Gisbergen, S. J. A.; Baerends, E. J. *J. Chem. Phys.* **2002**, *116*, 6930−6940.

(27) Wang, Y.; Raabe, G.; Repges, C.; Fleischhauer, J. *Int. J. Quantum Chem.* **2003**, *93*, 265−270.

(28) Stephens, P. J.; McCann, D. M.; Devlin, F. J.; Cheeseman, J. R.; Frisch, M. J. *J. Am. Chem. Soc.* **2004**, *126*, 7514−7521.

(29) Pecul, M.; Ruud, K.; Helgaker, T. *Chem. Phys. Lett.* **2004**, *388*, 110−119.

(30) Gorelsky, S. I.; Lever, A. B. P. *J. Organomet. Chem.* **2001**, *635*, 187−196.

(31) Rosa, A.; Ricciardi, G.; Gritsenko, O.; Baerends, E. J. Excitation energies of metal complexes with time-dependent density functional theory. In *Principles and Applications of Density Functional Theory in Inorganic Chemistry I*; Kaltsoyannis, N., McGrady, J. E., Eds.; Springer: Heidelberg, Germany, 2004; Vol. 112.

(32) Jorge, F. E.; Autschbach, J.; Ziegler, T. *J. Am. Chem. Soc.* **2005**, *127*, 975−985.
(33) Brown, A.; Kemp, C. M.; Mason, S. F. *J. Chem. Soc.* (*A*) **1971**, 751−755.
(34) Casida, M. E.; Gutierrez, F.; Guan, J.; Gadea, F.-X.; Salahub, D. R.; Daudey, J.-P. *J. Chem. Phys.* **2000**, *113*, 7062−7071.
(35) Balzani, V.; Juris, A.; Venturi, M.; Campagna, S.; Serroni, S. *Chem. Rev.* **1996**, *96*, 759−833.
(36) Damrauer, N. H.; Cerullo, G.; Yeh, A.; Boussie, T. R.; Shank, C. V.; McCusker, J. K. *Science* **1997**, *275*, 54−57.
(37) Ortmans, I.; Moucheron, C.; Kirsch-De Mesmaeker, A. *Coord. Chem. Rev.* **1998**, *168*, 233−271.
(38) McCusker, J. K. *Acc. Chem. Res* **2003**, *36*, 876−887.
(39) Pourtois, G.; Belionne, D.; Moucheron, C.; Schumm, S.; Kirsch-De Mesmaeker, A.; Lazzaroni, R.; Bredas, J.-L. *J. Am. Chem. Soc.* **2004**, *126*, 683−692.
(40) Gao, F. G.; Bard, A. J. *J. Am. Chem. Soc.* **2000**, *122*, 7426−7427.
(41) Hagfeldt, A.; Gratzel, M. *Chem. Rev.* **1995**, *95*, 49−68.
(42) Klimant, I.; Wolfbeis, O. S. *Anal. Chem.* **1995**, *67*, 3160−3166.
(43) Erkkila, K. E.; Odom, D. T.; Barton, J. K. *Chem. Rev.* **1999**, *99*, 2777−2795.
(44) Armistead, P. M.; Thorp, H. H. *Bioconj. Chem.* **2002**, *13*, 172−176.
(45) Kirsch-De Mesmaeker, A.; Lecomte, J. P.; Kelly, J. M. *Top. Curr. Chem.* **1996**, *177*, 25−76.
(46) Barton, J. K. *Science* **1986**, *233*, 727−734.
(47) Sundquist, W. I.; Lippard, S. J. *Coord. Chem. Rev.* **1990**, *100*, 293−322.
(48) Pauly, M.; Kayser, I.; Schmitz, M.; Dicato, M.; Del Guerzo, A.; Kolber, I.; Moucheron, C.; Kirsch-De Mesmaeker, A. *Chem. Commun.* **2002**, 1086−1087.
(49) van Lenthe, E.; Baerends, E. J.; Snijders, J. G. *J. Chem. Phys.* **1993**, *99*, 4597−4610.
(50) Dyall, K.; van Lenthe, E. *J. Chem. Phys.* **1999**, *111*, 1366−1372.
(51) Fonseca Guerra, C.; Visser, O.; Snijders, J. G.; te Velde, G.; Baerends, E. J. Parallelisation of the Amsterdam Density Functional Program. In *Methods and Techniques for Computational Chemistry*; STEF: Cagliari, 1995.
(52) te Velde, G.; Bickelhaupt, F. M.; Baerends, E. J.; van Gisbergen, S. J. A.; Fonseca Guerra, C.; Snijders, J. G.; Ziegler, T. *J. Comput. Chem.* **2001**, *22*, 931−967.
(53) Baerends, E. J. et al. Amsterdam Density Functional, Theoretical Chemistry, Vrije Universiteit, Amsterdam, URL http://www.scm.com.
(54) Autschbach, J.; Ziegler, T. *J. Chem. Phys.* **2002**, *116*, 891−896.
(55) Autschbach, J.; Ziegler, T.; Patchkovskii, S.; van Gisbergen, S. J. A.; Baerends, E. J. *J. Chem. Phys.* **2002**, *117*, 581−592.
(56) van Gisbergen, S. J. A.; Snijders, J. G.; Baerends, E. J. *J. Chem. Phys.* **1995**, *103*, 9347−9354.
(57) van Gisbergen, S. J. A.; Snijders, J. G.; Baerends, E. J. *Comput. Phys. Commun.* **1999**, *118*, 119−138.
(58) van Gisbergen, S. J. A.; Fonseca-Guerra, C.; Baerends, E. J. *J. Comput. Chem.* **2000**, *21*, 1511−1523.
(59) Ditchfield, R. *Mol. Phys.* **1974**, *27*, 789−807.
(60) Grimme, S. *Chem. Phys. Lett.* **2001**, *339*, 380−388.
(61) URL: http://www.nsm.buffalo.edu/∼jochena.
(62) Frantz, J. g3data, 2002; URL: http://beam.helsinki.fi/∼frantz/software/g3data.php.
(63) Turbomole, Ver. 5.6; Quantum Chemistry Group, Universitaet Karlsruhe.
(64) Furche, F. *J. Chem. Phys.* **2001**, *114*, 5982−5992.
(65) Furche, F.; Ahlrichs, R. *J. Chem. Phys.* **2001**, *114*, 10362−10367.
(66) Andrae, D.; Haeussermann, U.; Dolg, M.; Stoll, H.; Preuss, H. *Theor. Chim. Acc.* **1990**, *77*, 123.
(67) Vosko, S. H.; Wilk, L.; Nusair, M. *Can. J. Phys.* **1980**, *58*, 1200−1211.
(68) Becke, A. D. *Phys. Rev. A* **1988**, *38*, 3098−3100.
(69) Perdew, J. P. *Phys. Rev. B* **1986**, *33*, 8822−8824.
(70) Perdew, J. P.; Chevary, J. A.; Vosko, S. H.; Jackson, K. A.; Pederson, M. R.; Singh, D. J.; Fiolhais, C. *Phys. Rev. B* **1992**, *46*, 6671−6687.
(71) Perdew, J. P.; Burke, K.; Ernzerhof, M. *Phys. Rev. Lett.* **1996**, *77*, 3865−3868.
(72) Zhang, Y.; Yang, W. *Phys. Rev. Lett.* **1998**, *80*, 890.
(73) Perdew, J. P.; Burke, K.; Ernzerhof, M. *Phys. Rev. Lett.* **1998**, *80*, 891.
(74) Hammer, B.; Hansen, L. B.; Norskov, J. K. *Phys. Rev. B* **1999**, *59*, 7413−7421.
(75) Schipper, P. R. T.; Gritsenko, O. V.; van Gisbergen, S. J. A.; Baerends, E. J. *J. Chem. Phys.* **2000**, *112*, 1344−1352.
(76) Della Sala, F.; Görling, A. *J. Chem. Phys.* **2001**, *115*, 5718.
(77) Della Sala, F.; Görling, A. *J. Chem. Phys.* **2002**, *116*, 5374.
(78) Gritsenko, O. V.; Baerends, E. J. *Phys. Rev. A* **2001**, *64*, 042506.
(79) Grüning, M.; Gritsenko, O. V.; Baerends, E. J. *J. Chem. Phys.* **2002**, *116*, 6435.
(80) Casida, M. E. Time-dependent density functional response theory for molecules. In *Recent advances in density functional methods*; Chong, D. P., Ed.; World Scientific: Singapore, 1995; Vol. 1.
(81) Flükiger, P.; Lüthi, H. P.; Portmann, S.; Weber, J. MOLEKEL 4.3; Swiss Center for Scientific Computing: Manno, Switzerland, 2000−2002.
(82) Portmann, S.; Lüthi, H. P. *CHIMIA* **2000**, *54*, 766−770.
(83) Bühl, M. *Chem. Phys. Lett.* **1997**, *267*, 251−257.
(84) Autschbach, J. The calculation of NMR parameters in transition metal complexes. In *Principles and Applications of Density Functional Theory in Inorganic Chemistry I*; Kaltsoyannis, N., McGrady, J. E., Eds.; Springer: Heidelberg, Germany, 2004; Vol. 112.
(85) Rinderspacher, B. C.; Schreiner, P. R. *J. Phys. Chem. A* **2004**, *108*, 2867−2870.
(86) Koh, L. L.; Xu, Y.; Hsieh, A. K.; Song, B.; Wu, F.; Ji, L. *Acta Crystallogr.* **1994**, *C50*, 884−886.
(87) Zalkin, A.; Templeton, D. H.; Ueki, T. *Inorg. Chem.* **1973**, *12*, 1641−1646.
(88) Hieringer, W.; Görling, A.; Arbouznikov, A.; Kaupp, M. To be submitted for publication.
(89) Klamt, A.; Schüürmann, G. *J. Chem. Soc., Perkin Trans. 2* **1993**, 799−805.
(90) Pye, C. C.; Ziegler, T. *Theor. Chim. Acc.* **1999**, *101*, 396−408.
(91) Jensen, L.; van Duijnen, P. T.; Snijders, J. *J. Chem. Phys.* **2003**, *119*, 3800−3809.
(92) Autschbach, J.; Jensen, L.; Swart, M. Manuscript in preparation.